In Vivo Evaluation of ^{18}F-SiFA*lin*–Modified TATE: A Potential Challenge for ^{68}Ga-DOTATATE, the Clinical Gold Standard for Somatostatin Receptor Imaging with PET

Sabrina Niedermoser[1], Joshua Chin[2], Carmen Wängler[3], Alexey Kostikov[2], Vadim Bernard-Gauthier[2,4], Nils Vogler[5], Jean-Paul Soucy[2,6], Alexander J. McEwan[4], Ralf Schirrmacher[2,4], and Björn Wängler[1]

[1]Division of Molecular Imaging and Radiochemistry, Department of Clinical Radiology and Nuclear Medicine, Medical Faculty Mannheim of Heidelberg University, Mannheim, Germany; [2]McConnell Brain Imaging Centre, Montreal Neurological Institute, McGill University, Montreal, Canada; [3]Division of Biomedical Chemistry, Department of Clinical Radiology and Nuclear Medicine, Medical Faculty Mannheim of Heidelberg University, Mannheim, Germany; [4]Division of Oncological Imaging, Department of Oncology, University of Alberta, Edmonton, AB, Canada; [5]Division of Nuclear Medicine, Department of Clinical Radiology and Nuclear Medicine, Medical Faculty Mannheim of Heidelberg University, Mannheim, Germany; and [6]Concordia–PERFORM Centre, Concordia University, Montreal, Canada

Radiolabeled peptides for tumor imaging with PET that can be produced with kits are currently in the spotlight of radiopharmacy and nuclear medicine. The diagnosis of neuroendocrine tumors in particular has been a prime example for the usefulness of peptides labeled with a variety of different radionuclides. Among those, ^{68}Ga and ^{18}F stand out because of the ease of radionuclide introduction (e.g., ^{68}Ga isotope) or optimal nuclide properties for PET imaging (slightly favoring the ^{18}F isotope). The in vivo properties of good manufacturing practice–compliant, newly developed kitlike-producible ^{18}F-SiFA– and ^{18}F-SiFA*lin*– (SiFA = silicon-fluoride acceptor) modified TATE derivatives were compared with the current clinical gold standard ^{68}Ga-DOTATATE for high-quality imaging of somatostatin receptor–bearing tumors. **Methods:** SiFA- and SiFA*lin*-derivatized somatostatin analogs were synthesized and radiolabeled using cartridge-based dried ^{18}F and purified via a C18 cartridge (radiochemical yield 49.8% ± 5.9% within 20–25 min) without high-performance liquid chromatography purification. Tracer lipophilicity and stability in human serum were tested in vitro. Competitive receptor binding affinity studies were performed using AR42J cells. The most promising tracers were evaluated in vivo in an AR42J xenograft mouse model by ex vivo biodistribution and in vivo PET/CT imaging studies for evaluation of their pharmacokinetic profiles, and the results were compared with those of the current clinical gold standard ^{68}Ga-DOTATATE. **Results:** Synthetically easily accessible ^{18}F-labeled silicon-fluoride acceptor–modified somatostatin analogs were developed. They exhibited high binding affinities to somatostatin receptor–positive tumor cells (1.88–14.82 nM). The most potent compound demonstrated comparable pharmacokinetics and an even slightly higher absolute tumor accumulation level in ex vivo biodistribution studies as well as higher tumor standardized uptake values in PET/CT imaging than ^{68}Ga-DOTATATE in vivo. The radioactivity uptake in nontumor tissue was higher than for ^{68}Ga-DOTATATE. **Conclusion:** The introduction of the novel SiFA building block SiFA*lin* and of hydrophilic auxiliaries enables a favorable in vivo biodistribution profile of the modified TATE peptides, resulting in high tumor-to-background ratios although lower than those observed with ^{68}Ga-DOTATATE. As further advantage, the SiFA methodology enables a kitlike labeling procedure for ^{18}F-labeled peptides advantageous for routine clinical application.

Key Words: ^{68}Ga-DOTATATE; PET; kitlike ^{18}F labeling; ^{18}F-SiFA*lin*-TATE; somatostatin receptor imaging

J Nucl Med 2015; 56:1100–1105
DOI: 10.2967/jnumed.114.149583

Radiolabeled peptides have emerged as valuable imaging tools for PET, although their clinical availability is still limited (*1*). These peptides are mostly labeled with radiometals such as ^{68}Ga and ^{64}Cu but also with ^{18}F (*2–6*). Although ^{68}Ga-labeled peptides exhibit favorable properties in clinical routine imaging, the resolution of the obtained PET images and thus sensitivity could be further improved using ^{18}F (*7*). Even more importantly, the widespread availability of ^{18}F would make such tracers more accessible. Furthermore, the availability and clinical use of ^{68}Ga-based tracers have been less than optimal because of the limited availability of the generators and their uncertain regulatory status. As there is an urgent demand in clinical diagnostic oncology for tumor-specific radiolabeled compounds depicting even very small tumors and metastases to compensate for the shortcomings of ^{18}F-FDG (*8,9*), the development of ^{18}F-labeled peptides is worth exploring. ^{18}F represents one of the most attractive radionuclides because of its accessibility and low positron energy allowing for high-resolution in vivo images. However, only a few clinical PET imaging sites routinely offer ^{18}F-radiolabeled peptides as a result of the typically difficult radiochemistry involved in peptide labeling with ^{18}F (*10,11*). Therefore, new labeling approaches have been developed, especially over the last decade (*12–16*). One of these approaches takes advantage of the thermodynamically favored formation of silicon-^{18}F bonds (silicon-fluoride acceptor [SiFA] chemistry, Fig. 1) (*17–23*). However, in vitro and in vivo studies revealed

Received Oct. 6, 2014; revision accepted Apr. 30, 2015.
For correspondence or reprints contact either of the following:
Ralf Schirrmacher, Department of Oncology, Division of Oncological Imaging, University of Alberta, 11560 University Ave., Edmonton, AB, Canada, T6G 1Z2.
E-mail: schirrma@ualberta.ca
Björn Wängler, Division of Molecular Imaging and Radiochemistry, Department of Clinical Radiology and Nuclear Medicine, Medical Faculty Mannheim of Heidelberg University, 68167 Mannheim, Germany.
E-mail: Bjoern.Waengler@medma.uni-heidelberg.de
Published online May 14, 2015.

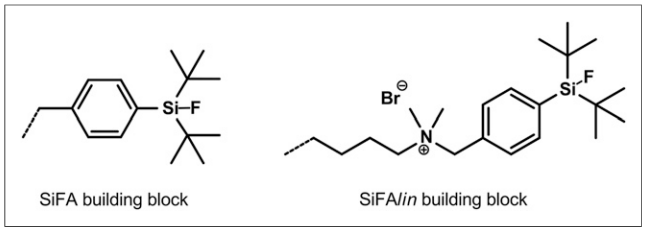

FIGURE 1. Structures of building blocks SiFA and SiFA*lin*.

inherent difficulties for its in vivo applicability: the unalterably high lipophilicity of the silicon-containing building block necessary for the in vivo stability of the Si-^{18}F bond leads to changes in the pharmacokinetic properties of the accordingly derivatized peptides (*19,24*). Nevertheless, the radiolabeling of SiFA is exceptionally mild, proceeds without forming side products, and can be performed by even untrained personnel (*17*), rendering this technique ideally suited for a kit-labeling approach similar to ^{99m}Tc radiochemistry for SPECT imaging.

To reduce the lipophilicity of SiFA-modified peptides, hydrophilic linkers and amino acids such as aspartic acid were introduced into the peptide sequence in this study together with a SiFA building block containing a permanent positive charge: SiFA*lin* (Figs. 1 and 2) (*25,26*). Most recently, Perrin's group introduced ^{18}F-AMBF$_3$-TATE for somatostatin receptor (SSTR) imaging, proving that a supposedly noncanonical labeling methodology based on isotopic exchange on trifluoroborates delivers an imaging agent of high specific activity and promising in vivo characteristics (Fig. 2) (*27*).

The main goal of our study was to prove the applicability of the SiFA approach for the labeling of clinically relevant peptides by developing a SiFA*lin*-derivatized Tyr^3-octreotate (TATE) that matches or surpasses the targeting ability of the current gold standard ^{68}Ga-DOTATATE (Fig. 2) for SSTR in vivo imaging with PET, thus overcoming ^{68}Ga limitations in terms of availability and image resolution.

MATERIALS AND METHODS

Chemistry

Synthesis of Peptides by Solid-Phase Peptide Synthesis. SiFA- and SiFA*lin*-derivatized somatostatin analogs were synthesized as described earlier (*17,28*). Details can be found in the supplemental information (supplemental materials are available at http://jnm.snmjournals.org).

^{18}F-Fluoride Radiolabeling and Quality Control of Peptides. The radiolabeling procedure was performed as previously described (*17*). In brief, aqueous ^{18}F-F$^-$ was trapped on a cartridge (Sep-Pak Accell Plus QMA Carbonate light, 46 mg; Waters) and dried with 20 mL of air and then rinsed with dry acetonitrile. Subsequently, a lyophilized mixture containing 110 μmol Kryptofix 2.2.2 (Merck) and 100 μmol KOH was dissolved in dry acetonitrile (500 μL). This freshly prepared solution was then used to elute the dried ^{18}F-F$^-$ from the cartridge (*17,29*). To the ^{18}F solution, 25 μL of a 1 M solution of oxalic acid in dry acetonitrile and a solution of 25 nmol of the precursor peptide were added. The isotopic exchange radiolabeling reaction proceeded within 5 min at ambient temperature with 70%–90% ^{18}F-fluoride incorporation. The reaction was quenched by the addition of 9 mL of 0.1 M HEPES (*N*-[2-hydroxyethyl]piperazine-*N*′-[2-ethanesulfonic acid]) buffer (pH 2) to receive the product in an aqueous acidic solution of approximately pH 5, which was subsequently purified with a Sep-Pak C18 cartridge. After the product was trapped, reactants and solvent were removed by washing the cartridge with water for injection. After elution of the purified product peptide with 200–500 μL of ethanol, the solution was diluted with isotonic saline to a final ethanol concentration of 10% or less and sterile-filtered. Analytic radio–high-performance liquid chromatography showed a radiochemical purity of 98% or greater.

In Vitro Characterization of Radiotracers

Determination of Lipophilicities. Two microliters of the product solution were added to 800 μL n-octanol and 800 μL of phosphate buffer (0.05 M, pH 7.4). After vigorous shaking for 5 min, the phases were separated by centrifugation at 14,000*g* for 2 min. Three aliquots of 100 μL of each phase were measured in a γ counter (*27*).

Determination of Serum Stabilities. Two hundred microliters of the injectable peptide solution were mixed with 500 μL of human serum and incubated over a period of 120 min at 37°C. After 10, 30, 60, and 120 min, aliquots of 5 μL were withdrawn and analyzed by analytic radio–high-performance liquid chromatography. The analyses indicated an unaltered radiochemical purity of all tracers of 98% or greater after 120 min in human serum.

Competitive Receptor Binding Affinity Studies. A competitive receptor binding assay using viable AR42J cells (10^5 cells per well, cell culture is described in the supplemental information) was performed. The cells were incubated with 0.5 nM ^{177}Lu-DOTATATE (preparation protocol is available in the supplemental information) in the presence of different concentrations of each SiFA-derivatized peptide (0–250 nM) dissolved in binding buffer (containing 10 mM $MgCl_2$, 1 mM $CaCl_2$, 25 mM HEPES, 0.5% bovine serum albumin, pH 7.4) for 60 min at ambient temperature with gentle agitation. The removal of binding buffer and washing steps (2 × 100 μL and 1 × 200 μL ice-cold phosphate-buffered saline) were performed using a multiscreen vacuum manifold (Millipore). Subsequently, the cell-bound and internalized radioactivity was measured using a γ counter (Cobra Quantum; Packard Canberra), and the inhibitory concentrations (IC_{50} values) were calculated using a nonlinear regression algorithm (GraphPad Prism; GraphPad Software). The experiments were each performed in triplicate.

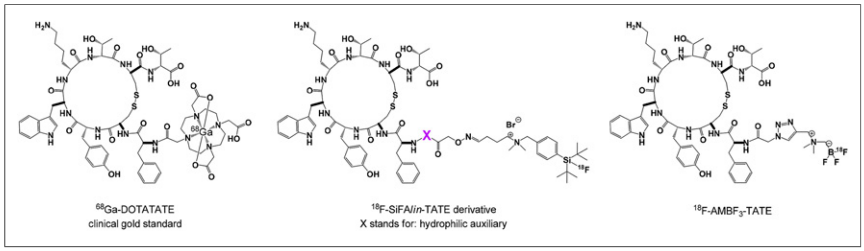

FIGURE 2. Structures of ^{68}Ga-DOTATATE, ^{18}F-SiFA*lin* analogs (X = site of introduction of hydrophilic auxiliaries for optimizing in vivo biodistribution properties), and ^{18}F-trifluoroborate derivative ^{18}F-AMBF$_3$-TATE.

In Vivo Characterization of Radiotracers

All animal experiments respected German animal protection laws and protocols of the local committee.

Biodistribution Experiments. Injectable solutions (50 μL) containing 1.1–5.3 MBq of the respective radiolabeled peptide were injected intravenously. Animals (4–10/group) bearing AR42J tumors (details can be found in the supplemental information) were sacrificed after 60

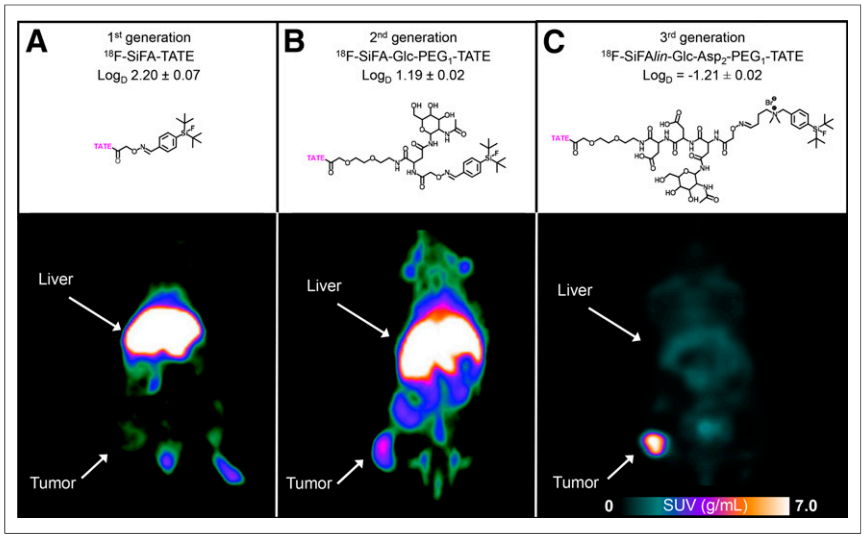

FIGURE 3. Small-animal PET images of 3 generations of SiFA-derivatized somatostatin analogs evaluated in AR42J tumor–bearing rodents. All images show coronal slices of the 50–90 min postinjection time frame. (A) ^{18}F-SiFA-TATE (^{18}F-**1**) in vivo images were obtained using a Philips Mosaic small-animal PET scanner. (B) ^{18}F-SiFA-Glc-PEG$_1$-TATE (^{18}F-**3**) images were obtained with a Siemens Inveon small-animal PET-scanner. (C) Images of ^{18}F-SiFA*lin*-Glc-Asp$_2$-PEG$_1$-TATE (^{18}F-**9**) distribution were obtained using a Bruker Albira small-animal PET/SPECT/CT scanner, indicating both a renal clearance and high activity accumulation in the SSTR-positive tumor tissue.

or 90 min, and the organs were dissected. After determination of organ weight, the activity of the tissues was measured using a γ counter (Wizard^2 2480; PerkinElmer) along with standards taken from the injected solution to determine the total injected activity. In blocking experiments, 200 μg of DOTATATE were coadministered together with the radiotracer.

Animal PET Imaging Studies. Nine tumor-bearing mice were injected with 4–8 MBq of the respective radiolabeled peptide (^{18}F-**9,** $n = 5$, and ^{68}Ga-DOTATATE, $n = 4$). A dynamic scan over 90 min and a subsequent CT image were acquired using a triple-modality Bruker Albira small-animal PET/SPECT/CT scanner.

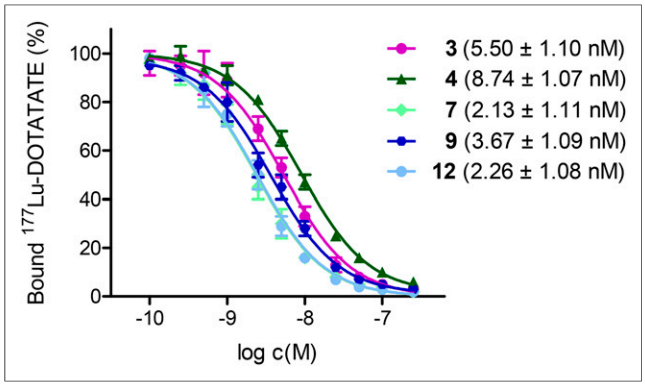

FIGURE 4. High tolerance of SSTR binding affinities of Tyr^3-octreotate toward hydrophilic chemical modifications without loss of bioactive potency. Binding affinities of third-generation SiFA (green, PEG$_1$: **4** and PEG$_5$: **7**) and SiFA*lin* (blue, PEG$_1$: **9** and PEG$_5$: **12**) derivatives compared with second-generation (magenta, **3**) were determined by competitive receptor binding affinity studies using AR42J cells and ^{177}Lu-DOTATATE as competitor. After incubation for 60 min in buffer at ambient temperature and successive washing steps, both cell-bound and internalized activity were measured using a γ counter. All experiments were performed in triplicate (error bars, mean ± SD).

RESULTS

SiFA Labeling Chemistry

Former studies introducing the SiFA labeling chemistry (first-generation SiFA-TATE (*19*) [^{18}F-**1**] and a less lipophilic second-generation compound SiFA-Glc-PEG$_1$-TATE (*17*) [^{18}F-**3**], Fig. 3) for convenient, fast, and facile peptide labeling of somatostatin analogs already demonstrated a high ^{18}F-fluoride incorporation within 5–10 min at ambient temperature. In in vivo scans, however, a pronounced liver uptake of ^{18}F-**1** and hardly any radioactivity accumulation in tumor tissue was observed (Fig. 3A) because of the highly lipophilic character of the SiFA synthon. The introduction of a carbohydrate moiety (*30*) and a PEG$_1$ linker (*26*) did not fully compensate for the SiFA lipophilicity, although a much higher amount of the labeled ^{18}F-**3** was found in tumor tissue (Fig. 3B).

To obtain more hydrophilic SiFA-bearing TATE derivatives better suitable for in vivo imaging of somatostatin-positive tumors due to more favorable pharmacokinetic properties, we introduced different hydrophilic auxiliaries into the peptide sequence and studied their influence on the tracer pharmacokinetics in vivo (*26*).

Chemical and Radiosyntheses

The synthesis of the TATE derivatives was performed using standard Fmoc solid-phase peptide synthesis protocols (*31*) (the supplemental information provides details). Besides a carbohydrate moiety, we introduced additional hydrophilic auxiliaries such as PEGs (polyethylene glycols) of different lengths, 1 or 2 aspartic acids, and a permanently positively charged SiFA*lin* synthon based on a previously described charged SiFA building block (Fig. 1) (*25*).

The purification of the labeled peptides proved to be simple with a C18 cartridge purification. The ^{18}F-labeled peptides were obtained in high radiochemical yields of 49.8% ± 5.9% ($n = 20$) and chemical as well as radiochemical purities of 98% or greater in only 20–25 min total synthesis time. This convenient 1-step ^{18}F-fluoride labeling strategy for peptides, proceeding with high efficiency and reliability, yields the ^{18}F-radiolabeled peptides with excellent specific activities of 44–63 GBq/μmol using starting activities of 3.3–6.7 GBq.

In Vivo Stability and Lipophilicity Determination

In accordance with previous studies, we found comparable results regarding the high stability of ^{18}F-labeled SiFA- and SiFA*lin*-TATE derivatives in human serum at 37°C over 120 min, showing no degradation of the radiolabeled peptides. The log$_D$ values (log$_D$: n-octanol to water distribution coefficient determined in n-octanol/phosphate buffer, pH 7.4) of the ^{18}F-labeled peptides were determined to gauge the influence of the hydrophilic auxiliaries. A significantly reduced overall lipophilicity was found for all newly developed SiFA- and SiFA*lin*-derivatized somatostatin analogs, compared with first- and second-generation SiFA-TATE derivatives **1** and **3** (Supplemental Fig. 2). Interestingly, the aspartic acids play the pivotal role in decreasing the lipophilicity because neither the different PEG spacers

TABLE 1
Tumor-to-Blood and Tumor-to-Muscle Ratios for Tested Newly Developed ^{18}F-Labeled Peptides ^{18}F-**4,** ^{18}F-**7,** ^{18}F-**9,** and ^{18}F-**12** Obtained from Ex Vivo Biodistribution at 90 Minutes after Injection

Ratio	^{18}F-**4**	^{18}F-**9**	^{18}F-**7**	^{18}F-**12**
Tumor to blood	4.30 ± 0.26	57.58 ± 35.89	12.31 ± 4.19	74.42 ± 20.37
Tumor to muscle	33.31 ± 11.94	211.05 ± 143.38	94.12 ± 26.37	256.49 ± 61.17

nor the permanently positive charge at the SiFA moiety decreased the overall lipophilicity significantly.

In Vitro Receptor Affinity Studies

Although former studies displayed no loss of SSTR affinity (*28*) on chemical modification at the nonpharmacophoric *N*-terminus of the somatostatin analog TATE, a competitive cell-based affinity study was performed on viable rat pancreas carcinoma AR42J cells, known to overexpress SSTRs (*32*). The binding assay demonstrated excellent IC_{50} values in the low nanomolar range for the newly developed SiFA-TATE derivatives and thus a preserved binding affinity to SSTRs (Fig. 4; Supplemental Fig. 3).

Biodistribution Experiments of ^{18}F-SiFA-TATE Derivatives

To investigate the pharmacokinetic characteristics of the most promising ^{18}F-labeled candidates for in vivo tumor imaging, derivatives with 2 different PEG lengths (PEG_1 and PEG_5) and both SiFA-synthons (**4** and **7** bearing SiFA, **9** and **12** bearing SiFA*lin*) were chosen for a comparative biodistribution study in AR42J tumor–bearing xenograft mice. The obtained results were compared with the current clinical gold standard ^{68}Ga-DOTATATE.

Once tumor sizes reached 0.2–0.8 cm^3, solutions of the radiolabeled peptides ^{18}F-**4,** ^{18}F-**7,** ^{18}F-**9,** ^{18}F-**12** and ^{68}Ga-DOTATATE were injected intravenously.

For biodistribution studies, the mice were sacrificed at 60 and 90 min after injection, and radioactivity measurements of necropsy tissue samples were performed (results of 60 min after injection are provided in Supplemental Fig. 4). The results showed significantly higher tumor-to-organ ratios for the positively charged SiFA*lin* derivatives ^{18}F-**9** and ^{18}F-**12** than for their SiFA counterparts ^{18}F-**4** and ^{18}F-**7** (Supplemental Fig. 6). The same was found at 90 min after injection: despite slightly lower absolute tumor accumulations than ^{18}F-**4** and ^{18}F-**7,** the SiFA*lin* derivatives ^{18}F-**9** and ^{18}F-**12** showed significantly higher tumor-to-background ratios (Table 1), thus rendering them better-suited for tumor visualization in vivo. Interestingly, the tracers containing a PEG_5 linker demonstrated an almost 2-fold-higher uptake in physiologically SSTR-positive tissues although the tumor uptake of PEG_1- and PEG_5-comprising peptide derivatives were comparable, thus making ^{18}F-SiFA*lin*-Glc-Asp_2-PEG_1-TATE (^{18}F-**9**) the most promising of the newly developed radiotracers.

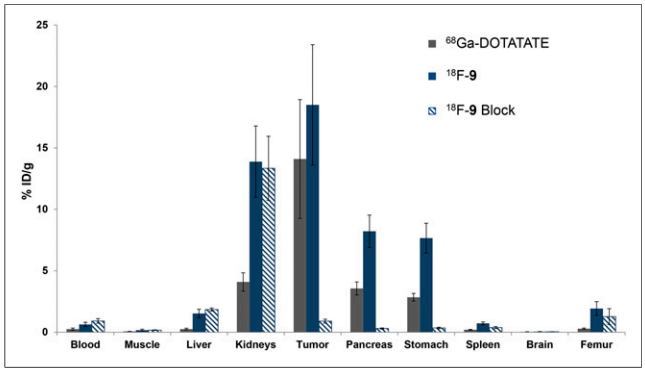

FIGURE 5. Results from ex vivo biodistribution studies comparing ^{68}Ga-DOTATATE (n = 5) with ^{18}F-**9** (n = 10) in AR42J tumor–bearing mice at 60 min after injection. Values are given as %ID/g. Most promising ^{18}F-SiFA*lin*-derivatized derivative ^{18}F-**9** demonstrates highly specific and even slightly higher tumor uptake than gold standard ^{68}Ga-DOTATATE. For ^{18}F-**9,** a blocking experiment using DOTATATE (200 μg/mouse; n = 5) was performed (dashed blue columns), showing specific binding of tracer to tumor and physiologically SSTR-positive tissues. ^{18}F-SiFA*lin* derivatives enable tumor-to-background ratios comparable to ^{68}Ga-DOTATATE.

When ^{18}F-**9** was compared with the clinically established gold standard ^{68}Ga-DOTATATE, evaluated under identical experimental conditions, ^{18}F-**9** demonstrated comparable pharmacokinetic properties (Fig. 5), displaying a high and specific tumor uptake and low nontarget organ accumulations. Those results demonstrate that ^{18}F-**9** is an interesting ^{18}F-labeled alternative to ^{68}Ga-DOTATATE, being as easily synthetically accessible as the latter, exhibiting more favorable physical decay characteristics such as a longer half-life and a significantly shorter maximum range of positrons.

To evaluate the potential of peptide ^{18}F-**9** for in vivo tumor imaging, an additional animal PET study was performed. The outcomes of this study are shown in Figure 3C, illustrating the evolution of SiFA-modified ^{18}F-labeled TATE derivatives with regard to their in vivo pharmacokinetics.

Furthermore, to directly compare the image qualities achievable using the clinical gold standard ^{68}Ga-DOTATATE and ^{18}F-**9,** a comparative small-animal PET/CT study in SSTR-positive tumor-bearing animals was performed and the results are shown in Figure 6.

These results demonstrate the high potential of newly developed compound ^{18}F-**9** for clinical in vivo imaging of neuroendocrine tumors with PET.

DISCUSSION

^{18}F-SiFA*lin*-Glc-Asp_2-PEG_1-TATE (^{18}F-**9**) was identified from among a variety of new synthetically easily accessible SiFA-modified TATE derivatives being evaluated for ^{18}F-labeled peptide-based SSTR imaging (Supplemental Fig. 1). ^{18}F-**9** demonstrated—as compared with the current clinical gold standard ^{68}Ga-DOTATATE—favorable in vivo pharmacokinetic properties with higher absolute tumor uptake, very good tumor–to–normal-tissue ratios, and excellent spatial resolution of the images. Nevertheless, higher binding by most normal tissue will likely decrease contrast with ^{18}F-9 in direct comparison to ^{68}Ga-DOTATATE.

Importantly, the radiosynthesis of ^{18}F-**9** was achieved within 20–25 min in a kitlike manner devoid of any special equipment or intricate purification procedures. The radiotracer was synthesized in radiochemical yields of 52.5% ± 4.9%, with specific activities of 44–63 GBq/μmol (1,200–1,700 Ci/mmol).

Similar to Perrin's synthesis of ^{18}F-$AMBF_3$-TATE, the SiFA*lin*-labeling approach maintained all the benefits of the trifluoroborate chemistry, again highlighting the advantages of ^{18}F-labeling

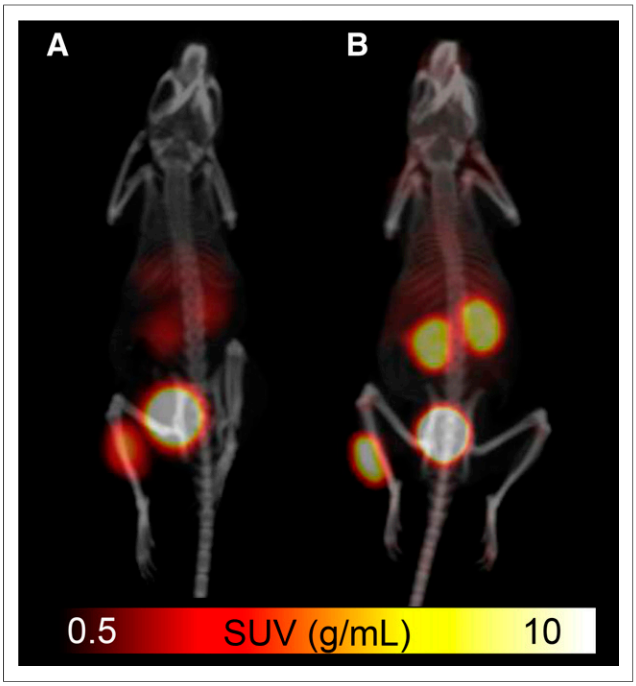

FIGURE 6. Comparative small-animal PET/CT imaging of SSTR-positive tumor-bearing mice using ^{68}Ga-DOTATATE (A) and ^{18}F-**9** (B) with identical standardized uptake value (SUV) scale for both images. Tumor accumulation SUVs in last frame (80–90 min after injection; showing highest accumulation of both tracers) are 5.50 for ^{68}Ga-DOTATATE and 7.80 for ^{18}F-**9.**

methods based on isotopic exchange (*27*). The introduction of aspartic acids into the TATE derivatives was the key to sufficiently reduce the overall lipophilicity of ^{18}F-**9** to a $\log_D$ of -1.21 ± 0.02. In addition, binding affinities of all SiFA*lin*- and auxiliary-modified peptides were in the nanomolar range, thus allowing for a strong interaction with the target receptors. The introduction of the novel SiFA building block SiFA*lin* (Fig. 1), characterized by a permanent positive charge, resulted in improved tumor-to-nontumor tissue ratios. These measures ultimately enabled a tumor-specific accumulation and renal clearance, which is mandatory for the overall quality of the resulting PET images. For ^{18}F-**9,** only renal excretion was observed in the AR42J tumor–bearing xenograft mouse model (Figs. 3C and 6B), with a maximum radioactivity accumulation in the tumor of 18.51 ± 4.89 percentage injected dose per gram (%ID/g) at 60 min after injection compared with 14.10 ± 4.84 %ID/g found for ^{68}Ga-DOTATATE under the same conditions as determined by ex vivo biodistribution experiments (Fig. 5). A higher accumulation of radioactivity in normal tissue might, however, be detrimental to the overall image quality. The in vivo resistance of ^{18}F-**9** to ^{18}F-hydrolysis is very high, as can be deduced from the low observed bone uptake of only 1.31 ± 0.31 %ID/g at 90 min after injection (Fig. 5).

Moreover, the SiFA*lin* structure seems to have a pronounced positive influence on the tumor-to-organ ratios as well as on the pathway of excretion. In the used xenograft tumor model, ^{18}F-**9** showed a promising biodistribution approaching the quality of ^{68}Ga-DOTATATE, which is a prerequisite for human application. In addition, the radioisotope ^{18}F has noteworthy physical advantages over other common radioisotopes used in SSTR imaging, yielding PET images of high resolution and quality, enabling a highly sensitive and efficient detection of neuroendocrine tumors. In studies in which quantification of uptake might be required, this approach is likely superior to that using ^{68}Ga-labeled peptides because of the significantly higher maximum energy of ^{68}Ga positrons as compared with those from ^{18}F (1,899 keV and 644 keV, respectively) (*33*). The longer half-life of ^{18}F is also a major advantage, as it will allow for distribution of the tracer over longer distances in the same manner as ^{18}F-FDG, to reach PET centers not equipped with a ^{68}Ge/^{68}Ga generator or able to locally perform ^{18}F-labeling.

The direct comparison of both tracers, ^{68}Ga-DOTATATE and ^{18}F-**9,** with PET/CT imaging of tumor-bearing animals (Fig. 6) shows the excellent image quality that can be obtained using the ^{18}F-labeled compound ^{18}F-**9,** in terms of not only image resolution but also absolute tumor uptake. However, if transferred to a human imaging situation in which the tumor is likely localized abdominally and not peripherally, as in the animal tumor model, the background activity will indeed be a potential liability for accurate tumor visualization.

The fact that the synthesis of the radiolabeled compounds takes place at room temperature within 5 min; is devoid of any HPLC purification; can be made fully compliant with good manufacturing practice protocols; and proceeds in a kitlike manner, yielding the final ^{18}F-labeled peptide in high radiochemical yields within 20–25 min only renders this new radiotracer highly attractive toward a clinical application. The final success of the atypical SiFA-labeling methodology using the optimized SiFA*lin* in a preclinical setting opens up new avenues for nuclear medicine diagnostic imaging based on ^{18}F-labeled peptide imaging agents.

For a new radiotracer to become a routine clinical tool, requirements include not only good science and clinical scale up, but also carefully conducted multicenter clinical trials, ubiquitous availability, regulatory approval, and clinical acceptance funding by insurers and providers. These goals are likely easier to achieve with an ^{18}F-labeled radiopharmaceutical with access to an extensive central radiopharmacy network than with a significantly-shorter-half-life generator-produced tracer, which cannot be delivered over longer distances. Our belief is that the ^{18}F-**9** tracer described in this article is an important step to achieving the goals identified herein. The kitlike formulation has the potential to make regulatory approval easier and ease acceptance by radiopharmacies. We propose to validate the safety and clinical efficacy of ^{18}F-**9** in future phase I and II clinical trials.

CONCLUSION

We presented the synthesis and in vitro and in vivo evaluation of an auxiliary-derivatized ^{18}F-SiFA*lin*-TATE for SSTR imaging in a preclinical AR42J mouse xenograft model. The synthesis was developed as a kitlike procedure yielding multiple doses of the tracer with high specific activity. In vitro binding assays confirmed the high binding affinity of the tracers toward SSTRs. The direct comparison of tracer ^{18}F-**9** with ^{68}Ga-DOTATATE in PET/CT imaging of tumor-bearing animals (Fig. 6) shows the excellent image quality, which can be obtained using the ^{18}F-labeled compound ^{18}F-**9** in terms of image resolution and absolute tumor uptake.

Ex vivo and in vivo biodistribution data obtained with small-animal PET/CT demonstrated the favorable pharmacokinetics and excellent tumor-to-nontarget tissue ratios in the preclinical mouse model, which warrant translation into human clinical trials.

DISCLOSURE

The costs of publication of this article were defrayed in part by the payment of page charges. Therefore, and solely to indicate this fact, this article is hereby marked "advertisement" in accordance with 18 USC section 1734. Funding for this study was provided by the German Research Foundation (WA 2132/3-1), the Bayern-Quebec-Allianz and the Ministry of Science, Research and the Arts of the State of Baden-Württemberg (AZ 42-04HV.M1412 (12)/1/1), and the National Science and Engineering Research Council of Canada (NSERC) (discovery grant). No other potential conflict of interest relevant to this article was reported.

ACKNOWLEDGMENTS

We thank Prof. Dr. Gerhard Glatting, Elisabeth Götz, Tobias Herzel, Sergej Losev, Dr. Flavia Molina, Dr. Mareike Roscher, and Anne-Maria Suhr for their excellent technical support.

REFERENCES

1. Smith G, Carroll L, Aboagye E. New frontiers in the design and synthesis of imaging probes for PET oncology: current challenges and future directions. *Mol Imaging Biol.* 2012;14:653–666.
2. Decristoforo C, Pickett RD, Verbruggen A. Feasibility and availability of ^{68}Ga-labelled peptides. *Eur J Nucl Med Mol Imaging*. 2012;39(suppl 1): S31–S40.
3. Ikotun OF, Lapi SE. The rise of metal radionuclides in medical imaging: copper-64, zirconium-89 and yttrium-86. *Future Med Chem.* 2011;3:599–621.
4. Coenen HH, Elsinga PH, Iwata R, et al. Fluorine-18 radiopharmaceuticals beyond [^{18}F]FDG for use in oncology and neurosciences. *Nucl Med Biol.* 2010;37:727–740.
5. Choyke PL. Science to practice: pilot study of FPPRGD2 for imaging $\alpha v\beta 3$ integrin—how integral are integrins? *Radiology.* 2011;260:1–2.
6. Li W, Meyer L, Anderson C. Radiopharmaceuticals for positron emission tomography imaging of somatostatin receptor positive tumors. In: Krause W, ed., *Contrast Agents III. Topics in Current Chemistry. 252*. Berlin: Springer; 2005:179–192.
7. Breeman WAP, de Blois E, Sze Chan H, Konijnenberg M, Kwekkeboom DJ, Krenning EP. ^{68}Ga-labeled DOTA-peptides and ^{68}Ga-labeled radiopharmaceuticals for positron emission tomography: current status of research, clinical applications, and future perspectives. *Semin Nucl Med.* 2011;41:314–321.
8. Adams S, Baum R, Rink T, Schumm-Dräger P-M, Usadel K-H, Hör G. Limited value of fluorine-18 fluorodeoxyglucose positron emission tomography for the imaging of neuroendocrine tumours. *Eur J Nucl Med.* 1998;25:79–83.
9. Ambrosini V, Tomassetti P, Franchi R, Fanti S. Imaging of NETs with PET radiopharmaceuticals. *Q J Nucl Med Mol Imaging.* 2010;54:16–23.
10. Wester HJ, Schottelius M. Fluorine-18 labeling of peptides and proteins. In: Schubiger PA, Lehmann L, Friebe M, eds., *PET Chemistry: Ernst Schering Research Foundation Workshop*. 64. Berlin: Springer; 2007:79–111.
11. Pretze M, Pietzsch D, Mamat C. Recent trends in bioorthogonal click-radiolabeling reactions using fluorine-18. *Molecules.* 2013;18:8618–8665.
12. McBride WJ, Sharkey RM, Karacay H, et al. A novel method of F-18 radiolabeling for PET. *J Nucl Med.* 2009;50:991–998.
13. Wan W, Guo N, Pan D, et al. First experience of ^{18}F-alfatide in lung cancer patients using a new lyophilized kit for rapid radiofluorination. *J Nucl Med.* 2013;54:691–698.
14. Smith GE, Sladen HL, Biagini SCG, Blower PJ. Inorganic approaches for radiolabelling biomolecules with fluorine-18 for imaging with positron emission tomography. *Dalton Trans.* 2011;40:6196–6205.
15. Ting R, Adam MJ, Ruth TJ, Perrin DM. Arylfluoroborates and alkylfluorosilicates as potential PET imaging agents: high-yielding aqueous biomolecular ^{18}F-labeling. *J Am Chem Soc.* 2005;127:13094–13095.
16. Liu Z, Li Y, Lozada J, et al. Kit-like ^{18}F-labeling of RGD-^{19}F-arytrifluroborate in high yield and at extraordinarily high specific activity with preliminary in vivo tumor imaging. *Nucl Med Biol.* 2013;40:841–849.
17. Wängler C, Niedermoser S, Chin JS, et al. One-step F-18-labeling of peptides for positron emission tomography imaging using the SiFA methodology. *Nat Protoc.* 2012;7:1946–1955.
18. Wängler B, Kostikov AP, Niedermoser S, et al. Protein labeling with the labeling precursor [^{18}F]SiFA-SH for positron emission tomography. *Nat Protoc.* 2012; 7:1964–1969.
19. Schirrmacher R, Bradtmöller G, Schirrmacher E, et al. F-18-labeling of peptides by means of an organosilicon-based fluoride acceptor. *Angew Chem Int Ed Engl.* 2006;45:6047–6050.
20. Mu L, Höhne A, Schubiger RA, et al. Silicon-based building blocks for one-step ^{18}F-radiolabeling of peptides for PET imaging. *Angew Chem Int Ed Engl.* 2008;47:4922–4925.
21. Dialer LO, Selivanova SV, Muller CJ, et al. Studies toward the development of new silicon-containing building blocks for the direct ^{18}F-labeling of peptides. *J Med Chem.* 2013;56:7552–7563.
22. Schulz J, Vimont D, Bordenave T, et al. Silicon-based chemistry: an original and efficient one-step approach to [^{18}F]-nucleosides and [^{18}F]-oligonucleotides for PET imaging. *Chemistry.* 2011;17:3096–3100.
23. Kostikov AP, Chin J, Orchowski K, et al. Synthesis of [^{18}F]SiFB: a prosthetic group for direct protein radiolabeling for application in positron emission tomography. *Nat Protoc.* 2012;7:1956–1963.
24. Höhne A, Mu L, Honer M, et al. Synthesis, F-18-labeling, and in vitro and in vivo studies of bombesin peptides modified with silicon-based building blocks. *Bioconjug Chem.* 2008;19:1871–1879.
25. Kostikov AP, Iovkova L, Chin J, et al. N-(4-(di-tert-butyl[F-18]fluorosilyl)benzyl)-2-hydroxy-N, N-dimethylethylammonium bromide ([F-18]SiFAN(+)Br(-)): a novel lead compound for the development of hydrophilic SiFA-based prosthetic groups for F-18-labeling. *J Fluor Chem.* 2011;132:27–34.
26. Hosseinimehr SJ, Tolmachev V, Orlova A. Liver uptake of radiolabeled targeting proteins and peptides: considerations for targeting peptide conjugate design. *Drug Discov Today.* 2012;17:1224–1232.
27. Liu Z, Pourghiasian M, Menard F, Pan J, Lin K-S, Perrin DM. Preclinical evaluation of a high-affinity ^{18}F-trifluoroborate octreotate derivative for somatostatin receptor imaging. *J Nucl Med.* 2014;55:1499–1505.
28. Wängler C, Waser B, Alke A, et al. One-step F-18-labeling of carbohydrate-conjugated octreotate-derivatives containing a silicon-fluoride-acceptor (SiFA): in vitro and in vivo evaluation as tumor imaging agents for positron emission tomography (PET). *Bioconjug Chem.* 2010;21:2289–2296.
29. Wessmann SH, Henriksen G, Wester HJ. Cryptate mediated nucleophilic F-18-fluorination without azeotropic drying. *Nuklearmedizin.* 2012;51:1–8.
30. Schottelius M, Wester H-J, Reubi JC, Senekowitsch-Schmidtke R, Schwaiger M. Improvement of pharmacokinetics of radioiodinated Tyr3-octreotide by conjugation with carbohydrates. *Bioconjug Chem.* 2002;13:1021–1030.
31. Wellings DA, Atherton E. Standard Fmoc protocols. *Methods Enzymol.* 1997;289:44–67.
32. Taylor JE, Theveniau MA, Bashirzadeh R, Reisine T, Eden PA. Detection of somatostatin receptor subtype-2 (Sstr2) in established tumors and tumor-cell lines: evidence for Sstr2 heterogeneity. *Peptides.* 1994;15:1229–1236.
33. Kemerink GJ, Visser MGW, Franssen R, et al. Effect of the positron range of ^{18}F, ^{68}Ga and ^{124}I on PET/CT in lung-equivalent materials. *Eur J Nucl Med Mol Imaging.* 2011;38:940–948.